1   **The novel coronavirus 2019 (2019-nCoV) uses the SARS-coronavirus receptor**

2   **ACE2 and the cellular protease TMPRSS2 for entry into target cells**

3

4   **Markus Hoffmann,[1*†] Hannah Kleine-Weber[1,2†], Nadine Krüger,[3,4] Marcel Müller,[5,6,7]**

5   **Christian Drosten,[5,6] Stefan Pöhlmann[1,2*]**

6

7   [1]Infection Biology Unit, German Primate Center – Leibniz Institute for Primate Research,

8   Göttingen, Germany

9   [2]Faculty of Biology and Psychology, University Göttingen, Göttingen, Germany

10   [3]Institute of Virology, University of Veterinary Medicine Hannover, Hannover, Germany.

11   [4]Research Center for Emerging Infections and Zoonoses, University of Veterinary Medicine

12   Hannover, Hannover, Germany.

13   [4]Charité-Universitätsmedizin Berlin, corporate member of Freie Universität Berlin, Humboldt-

14   Universität zu Berlin, and Berlin Institute of Health, Institute of Virology, Berlin, Germany.

15   [5]German Centre for Infection Research, associated partner Charité, Berlin, Germany.

16   [6]Martsinovsky Institute of Medical Parasitology, Tropical and Vector Borne Diseases, Sechenov

17   University, Moscow, Russia.

18

19   Corresponding authors. E-mail: mhoffmann@dpz.eu (M.H.), spoehlmann@dpz.eu (S.P.)

20   † These authors contributed equally

21

22

23

24   **Abstract: The emergence of a novel, highly pathogenic coronavirus, 2019-nCoV, in China,**

25   **and its rapid national and international spread pose a global health emergency.**

26   **Coronaviruses use their spike proteins to select and enter target cells and insights into**

27   **nCoV-2019 spike (S)-driven entry might facilitate assessment of pandemic potential and**

28   **reveal therapeutic targets. Here, we demonstrate that 2019-nCoV-S uses the SARS-**

29   **coronavirus receptor, ACE2, for entry and the cellular protease TMPRSS2 for 2019-nCoV-**

30   **S priming. A TMPRSS2 inhibitor blocked entry and might constitute a treatment option.**

31   **Finally, we show that the serum form a convalescent SARS patient neutralized 2019-nCoV-**

32   **S-driven entry. Our results reveal important commonalities between 2019-nCoV and**

33   **SARS-coronavirus infection, which might translate into similar transmissibility and disease**

34   **pathogenesis. Moreover, they identify a target for antiviral intervention.**

35

36   **One sentence summary:** The novel 2019 coronavirus and the SARS-coronavirus share central

37   biological properties which can guide risk assessment and intervention.

38

39

40

41

42

43

44

45

46

2

47 Several members of the family *Coronaviridae* constantly circulate in the human population and

48 usually cause mild respiratory disease (*1*). In contrast, the severe acute respiratory syndrome-

49 associated coronavirus (SARS-CoV) and the Middle East respiratory syndrome-associated

50 coronavirus (MERS-CoV) are transmitted from animals to humans and cause severe respiratory

51 diseases in afflicted human patients, SARS and MERS, respectively (*2*). SARS emerged in 2002

52 in Guangdong province, China, and its subsequent global spread was associated with 8096 cases

53 and 774 deaths (*3, 4*). The virus uses Chinese horseshoe bats as natural reservoir (*5, 6*) and is

54 transmitted via intermediate hosts to humans. Thus, SARS-CoV was identified in Civet cats and

55 raccoon dogs, which are sold as food sources in Chinese wet markets (*7*). No specific antivirals

56 or approved vaccines are available to combat SARS and the SARS pandemic in 2002/2003 was

57 stopped by conventional control measures, including travel restrictions and patient isolation.

58   In December 2019 a new infectious respiratory disease emerged in Wuhan, Hubei

59 province, China (*8-10*). Initial infections occurred at Huanan seafood market, potentially due to

60 animal contact. Subsequently, human-to-human transmission occurred (*11*)

61 and the disease rapidly spread within China. A novel coronavirus, 2019-nCoV, which is closely

62 related to SARS-CoV, was detected in patients and is believed to be the etiologic agent of the

63 new lung disease (*10*). On January 28, 2020, at total of 4593 laboratory confirmed infections

64 were reported, including 976 severe cases and 106 deaths (*12*). Infections were also detected in

65 14 countries outside China and were associated with international travel. At present, it is

66 unknown whether the sequence similarities between 2019-nCoV and SARS-CoV translate into

67 similar biological properties, including pandemic potential (*13*).

68   The spike (S) protein of coronaviruses facilitates viral entry into target cells. Entry

69 depends on S protein binding to a cellular receptor and on S protein priming by a cellular

70 protease. SARS-S engages angiotensin-converting enzyme 2 (ACE2) as entry receptor (*14*) and

3

71 employs the cellular serine protease TMPRSS2 for S protein priming (*15-17*). The SARS-

72 S/ACE2 interface has been elucidated and the efficiency of ACE2 usage was found to be a key

73 determinant of SARS-CoV transmissibility (*6, 18*). SARS-S und 2019-nCoV-S share ~76%

74 amino acid identity. However, it is unknown whether 2019-nCoV-S like SARS-S employs ACE2

75 and TMPRSS2 for host cell entry.

76   Replication-defective vesicular stomatitis virus (VSV) particles bearing coronavirus S

77 proteins faithfully reflect key aspects of coronavirus host cell entry (*19*). We employed VSV

78 pseudotypes bearing 2019-nCoV-S to study cell entry of 2019-nCoV. Both 2019-nCoV-S and

79 SARS-S were comparably expressed (Fig. 1A) and incorporated into VSV particles (Fig. 1B),

80 allowing a meaningful side-by-side comparison. We first focused on 2019-nCoV cell tropism.

81 Transduction of cell lines of animal and human origin revealed that all cell lines were readily

82 susceptible to entry driven by the pantropic VSV glycoprotein (VSV-G) (Fig. 1C), as expected.

83 (Fig. 1C). Notably, 2019-nCoV-S facilitated entry into an identical spectrum of cell lines as

84 SARS-S (Fig. 1C), suggesting similarities in receptor choice.

85   Sequence analysis revealed that 2019-nCoV clusters with SARS-CoV-related viruses

86 from bats (SARSr-CoV), of which some but not all can use ACE2 for host cell entry (Fig. 2A and

87 fig. S1). Analysis of the receptor binding motif (RBM), a portion of the receptor binding domain

88 (RBD) that makes contact with ACE2, revealed that most amino acid residues essential for ACE2

89 binding were conserved in 2019-nCoV-S but not in the S proteins of SARSr-CoV previously

90 found not to use ACE2 for entry (Fig. 2B). In agreement with these findings, directed expression

91 of human and bat ACE2 but not human DPP4, the entry receptor used by MERS-CoV (*20*), or

92 human APN, the entry receptor used by HCoV-229E (*21*), allowed 2019-nCoV-S- and SARS-S-

93 driven entry into otherwise non-susceptible BHK-21 cells (Fig. 2C), indicating that 2019-nCoV-S

94 like SARS-S uses ACE2 for cellular entry.

4

95   We next investigated protease dependence of 2019-nCoV entry. SARS-CoV can use the

96   endosomal cysteine proteases cathepsin B and L (CatB/L) for S protein priming in TMPRSS2$^-$

97   cell lines (22). However, TMPRSS2 is expressed in viral target cells in the lung (23) and entry

98   into TMPRSS2$^+$ cell lines is promoted by TMPRSS2 (15-17) and is partially CatB/L

99   independent, although blockade of both proteases is required for efficient entry inhibition (24).

100   Moreover, TMPRSS2 but not CatB/L activity is essential for spread of SARS-CoV and other

101   coronaviruses in the infected host (25, 26). For initial insights into 2019-nCoV-S protease choice,

102   we employed ammonium chloride, which elevates endosomal pH and thereby blocks CatB/L

103   activity. Ammonium chloride treatment blocked VSV-G-driven entry into both cell lines studied

104   while entry driven by the Nipah virus F and G proteins was not affected (Fig. 3A), in keeping

105   with expectations. Moreover, ammonium chloride treatment strongly inhibited 2019-nCoV-S-

106   and SARS-S-driven entry into TMPRSS2$^-$ 293T cells while inhibition of entry into TMPRSS2$^+$

107   Caco-2 cells was less efficient, which would be compatible with 2019-nCoV-S priming by

108   TMPRSS2 in Caco-2 cells. Indeed, the serine protease inhibitor camostat mesylate, which is

109   active against TMPRSS2 (24), efficiently blocked 2019-nCoV-S-driven entry into Caco-2

110   (TMPRSS2$^+$) but not 293T (TMPRSS2$^-$) cells while the CatB/L inhibitor E64d had the opposite

111   effect (Fig. 3B). Moreover, directed expression of TMPRSS2 rescued 2019-nCoV-S-driven entry

112   from inhibition by E64d (Fig. 3C), demonstrating that 2019-nCoV-S uses TMPRSS2 for priming.

113   Convalescent SARS patients exhibit a neutralizing antibody response directed against the

114   viral S protein (27). We investigated whether such antibodies block 2019-nCoV-S-driven entry.

115   Serum from a convalescent SARS patient inhibited SARS-S- but not VSV-G-driven entry in a

116   concentration dependent manner (Fig. 4). In addition, the serum reduced 2019-nCoV-S-driven

117   entry, although with somewhat lower efficiency as compared to SARS-S (Fig. 4). Thus, antibody

118   responses raised against SARS-S during infection or vaccination might offer some protection

119   against 2019-nCoV infection.

120   The finding that 2019-nCoV-S and SARS-S use the same receptor, ACE2, for entry into

121   target cells has important implications for our understanding of 2019-nCoV transmissibility and

122   pathogenesis. Thus, one can expect that 2019-nCoV targets the same cells as SARS-CoV and that

123   the previously documented modest ACE2 expression in the upper respiratory tract (*23, 28*) might

124   limit 2019-nCoV transmissibility. Moreover, it is noteworthy that ACE2 expression is not limited

125   to the lung and that extrapulmonary spread of SARS-CoV in $ACE2^+$ tissues was observed (*29,*

126   *30*). The same can be expected for 2019-nCoV, although affinity of SARS-S and 2019-nCoV-S

127   for ACE2 remains to be compared.

128   Priming of coronavirus S proteins by host cell proteases is essential for viral entry into

129   cells and protease choice can determine zoonotic potential (*31*). The S proteins of SARS-CoV

130   can use the endosomal cysteine proteases for S protein priming in TMPRSS2$^-$ cells (*22*).

131   However, S protein priming by TMPRSS2 but not CatB/L is essential for viral entry into primary

132   target cells and for viral spread in the infected host (*24-26*). The present study suggests that 2019-

133   nCoV spread might also depend on TMPRSS2 activity and it is noteworthy that the serine

134   protease inhibitor camostat mesylate blocks TMPRSS2 activity (*24, 26*) and has been approved in

135   Japan for human use, although for an unrelated indication. This compound or related ones should

136   be considered for treatment of 2019-nCoV infected patients.

137   Convalescent SARS patients exhibit a neutralizing antibody response that can be detected

138   even 24 months after infection (*27*) and this is largely directed against the S protein. Moreover,

139   experimental SARS vaccines, including recombinant S protein (*32*) and inactivated virus (*33*)

140   induce neutralizing antibody responses. Our results, although limited in significance due to a

141   single patient serum being available for testing, indicate that neutralizing antibody responses

142   raised against SARS-S should also offer some protection against 2019-nCoV infection, which

143   may have implications for outbreak control.

144

145

146

147

148

149

150

151

152

153

154

155

156

157

158

159

160

161

162

163

164

165

References and Notes

166

167   1.   V. M. Corman, J. Lienau, M. Witzenrath, [Coronaviruses as the cause of respiratory

168   infections]. *Internist (Berl)* **60**, 1136-1145 (2019).

169   2.   A. R. Fehr, R. Channappanavar, S. Perlman, Middle East Respiratory Syndrome:

170   Emergence of a Pathogenic Human Coronavirus. *Annu Rev Med* **68**, 387-399 (2017).

171   3.   W. H. Organization. (2004), vol. 2020.

172   4.   E. de Wit, N. van Doremalen, D. Falzarano, V. J. Munster, SARS and MERS: recent

173   insights into emerging coronaviruses. *Nat Rev Microbiol* **14**, 523-534 (2016).

174   5.   S. K. Lau *et al.*, Severe acute respiratory syndrome coronavirus-like virus in Chinese

175   horseshoe bats. *Proc Natl Acad Sci U S A* **102**, 14040-14045 (2005).

176   6.   F. Li, W. Li, M. Farzan, S. C. Harrison, Structure of SARS coronavirus spike receptor-

177   binding domain complexed with receptor. *Science* **309**, 1864-1868 (2005).

178   7.   Y. Guan *et al.*, Isolation and characterization of viruses related to the SARS coronavirus

179   from animals in southern China. *Science* **302**, 276-278 (2003).

180   8.   C. Wang, P. W. Horby, F. G. Hayden, G. F. Gao, A novel coronavirus outbreak of global

181   health concern. *Lancet*, (2020).

182   9.   C. Huang *et al.*, Clinical features of patients infected with 2019 novel coronavirus in

183   Wuhan, China. *Lancet*, (2020).

184   10.   N. Zhu *et al.*, A Novel Coronavirus from Patients with Pneumonia in China, 2019. *N Engl

185   J Med*, (2020).

186   11.   J. F. Chan *et al.*, A familial cluster of pneumonia associated with the 2019 novel

187   coronavirus indicating person-to-person transmission: a study of a family cluster. *Lancet*,

188   (2020).

189   12.   W. H. Organization. (2020), vol. 2020.

190   13.   V. J. Munster, M. Koopmans, N. van Doremalen, D. van Riel, E. de Wit, A Novel

191   Coronavirus Emerging in China - Key Questions for Impact Assessment. *N Engl J Med*,

192   (2020).

193   14.   W. Li *et al.*, Angiotensin-converting enzyme 2 is a functional receptor for the SARS

194   coronavirus. *Nature* **426**, 450-454 (2003).

195   15.   I. Glowacka *et al.*, Evidence that TMPRSS2 activates the severe acute respiratory

196   syndrome coronavirus spike protein for membrane fusion and reduces viral control by the

197   humoral immune response. *J Virol* **85**, 4122-4134 (2011).

198   16.   S. Matsuyama *et al.*, Efficient activation of the severe acute respiratory syndrome

199   coronavirus spike protein by the transmembrane protease TMPRSS2. *J Virol* **84**, 12658-

200   12664 (2010).

201   17.   A. Shulla *et al.*, A transmembrane serine protease is linked to the severe acute respiratory

202   syndrome coronavirus receptor and activates virus entry. *J Virol* **85**, 873-882 (2011).

203   18.   W. Li *et al.*, Receptor and viral determinants of SARS-coronavirus adaptation to human

204   ACE2. *EMBO J* **24**, 1634-1643 (2005).

205   19.   H. Kleine-Weber *et al.*, Mutations in the Spike Protein of Middle East Respiratory

206   Syndrome Coronavirus Transmitted in Korea Increase Resistance to Antibody-Mediated

207   Neutralization. *J Virol* **93**, (2019).

208   20.   V. S. Raj *et al.*, Dipeptidyl peptidase 4 is a functional receptor for the emerging human

209   coronavirus-EMC. *Nature* **495**, 251-254 (2013).

210   21.   C. L. Yeager *et al.*, Human aminopeptidase N is a receptor for human coronavirus 229E.

211   *Nature* **357**, 420-422 (1992).

212   22.   G. Simmons *et al.*, Inhibitors of cathepsin L prevent severe acute respiratory syndrome

213   coronavirus entry. *Proc Natl Acad Sci U S A* **102**, 11876-11881 (2005).

214   23.   S. Bertram *et al.*, Influenza and SARS-coronavirus activating proteases TMPRSS2 and
215   HAT are expressed at multiple sites in human respiratory and gastrointestinal tracts. *PLoS*
216   *One* **7**, e35876 (2012).

217   24.   M. Kawase, K. Shirato, L. van der Hoek, F. Taguchi, S. Matsuyama, Simultaneous
218   treatment of human bronchial epithelial cells with serine and cysteine protease inhibitors
219   prevents severe acute respiratory syndrome coronavirus entry. *J Virol* **86**, 6537-6545
220   (2012).

221   25.   N. Iwata-Yoshikawa *et al.*, TMPRSS2 Contributes to Virus Spread and Immunopathology
222   in the Airways of Murine Models after Coronavirus Infection. *J Virol* **93**, (2019).

223   26.   Y. Zhou *et al.*, Protease inhibitors targeting coronavirus and filovirus entry. *Antiviral Res*
224   **116**, 76-84 (2015).

225   27.   W. Liu *et al.*, Two-year prospective study of the humoral immune response of patients
226   with severe acute respiratory syndrome. *J Infect Dis* **193**, 792-795 (2006).

227   28.   I. Hamming *et al.*, Tissue distribution of ACE2 protein, the functional receptor for SARS
228   coronavirus. A first step in understanding SARS pathogenesis. *J Pathol* **203**, 631-637
229   (2004).

230   29.   J. Gu *et al.*, Multiple organ infection and the pathogenesis of SARS. *J Exp Med* **202**, 415-
231   424 (2005).

232   30.   Y. Ding *et al.*, Organ distribution of severe acute respiratory syndrome (SARS) associated
233   coronavirus (SARS-CoV) in SARS patients: implications for pathogenesis and virus
234   transmission pathways. *J Pathol* **203**, 622-630 (2004).

235   31.   V. D. Menachery *et al.*, Trypsin treatment unlocks barrier for zoonotic bat coronaviruses
236   infection. *J Virol*, (2019).

237   32.   Y. He, J. Li, S. Heck, S. Lustigman, S. Jiang, Antigenic and immunogenic

238   characterization of recombinant baculovirus-expressed severe acute respiratory syndrome

239   coronavirus spike protein: implication for vaccine design. *J Virol* **80**, 5757-5767 (2006).

240   33.   J. T. Lin *et al.*, Safety and immunogenicity from a phase I trial of inactivated severe acute

241   respiratory syndrome coronavirus vaccine. *Antivir Ther* **12**, 1107-1113 (2007).

242

243

244

245

246

247

248

249

250

251

252

253

254

255

256

257

258

259

260

270

271

272

273

274

275

276

277

278

279

280

281

282

283

284

285   **Supplementary Materials**

286   Figure S1

287

288   **Figure legends**

289

290   **Fig. 1. 2019-nCoV-S and SARS-S facilitates entry into a similar panel of mammalian cell**

291   **lines.** Analysis of 2019-nCoV-S expression (**A**) and pseudotype incorporation (**B**) by Western

292   blot. Representative blots from three experiments are shown. ß-Actin (cell lysates) and VSV-M

293   (particles) served as loading controls. (C) Cell lines of human and animal origin were inoculated

294   with pseudotyped VSV harboring VSV-G, SARS-S or 2019-nCoV-S. At 16 h postinoculation,

295   pseudotype entry was analyzed. Shown are the combined data of three experiments. Error bars

296   indicate SEM.

297

298   **Fig. 2. 2019-nCoV-S utilizes ACE2 as cellular receptor.** (**A**) The S protein of 2019-nCoV

299   clusters phylogenetically with S proteins of known bat-associated betacoronaviruses (see also SI

300   Figure 1 for more details). (**B**) Alignment of the receptor binding motif of SARS-S with

301   corresponding sequences of bat-associated betacoronavirus S proteins that are able or unable to

302   use ACE2 as cellular receptor reveals that 2019-nCoV possesses amino acid residues crucial for

303   ACE2 binding. (**C**) 293T cells transiently expressing ACE2 of human (dark blue) or bat (light

304   blue) origin, human APN (purple) or hDPP4 (green) were inoculated with pseudotyped VSV

305   harboring VSV-G, SARS-S, 2019-nCoV-S, MERS-S or 229E-S. At 16 h postinoculation,

306   pseudotype entry was analyzed. The average of three independent experiments is shown. Error

307   bars indicate SEM.

308

13

309 **Fig. 3. 2019-nCoV-S employs TMPRSS2 for S protein priming.** Ammonium chloride (**A**),

310 E64d (CatB/L inhibitor) (**B**) and/or camostat (TMPRSS2 inhibitor) (**B**) were added to the

311 indicated target cells before transduction with pseudotypes bearing the indicated glycoproteins.

312 (**C**) 293T cells transiently expressing ACE2 alone or in combination with TMPRSS2 were

313 incubated with CatB/L inhibitor E64d or PBS as control and inoculated with pseudotypes bearing

314 the indicated viral surface proteins. The average of three independent experiments is shown in

315 panels A-C. Error bars indicate SEM. Statistical significance was tested by two-way ANOVA

316 with Dunnett posttest.

317

318 **Fig. 4. Serum from a convalescent SARS patient cross-neutralizes 2019-nCoV-S-driven**

319 **entry.** Pseudotypes harboring the indicated viral surface proteins were incubated with different

320 dilutions of serum from a convalescent SARS patient and subsequently inoculated onto 293T

321 cells that transiently express ACE2 in order to evaluate cross-neutralization. The results from a

322 representative experiment with triplicate samples are shown and were confirmed in a separate

323 experiment. Error bars indicate SD. Statistical significance was tested by two-way ANOVA with

324 Dunnett posttest.

325

326
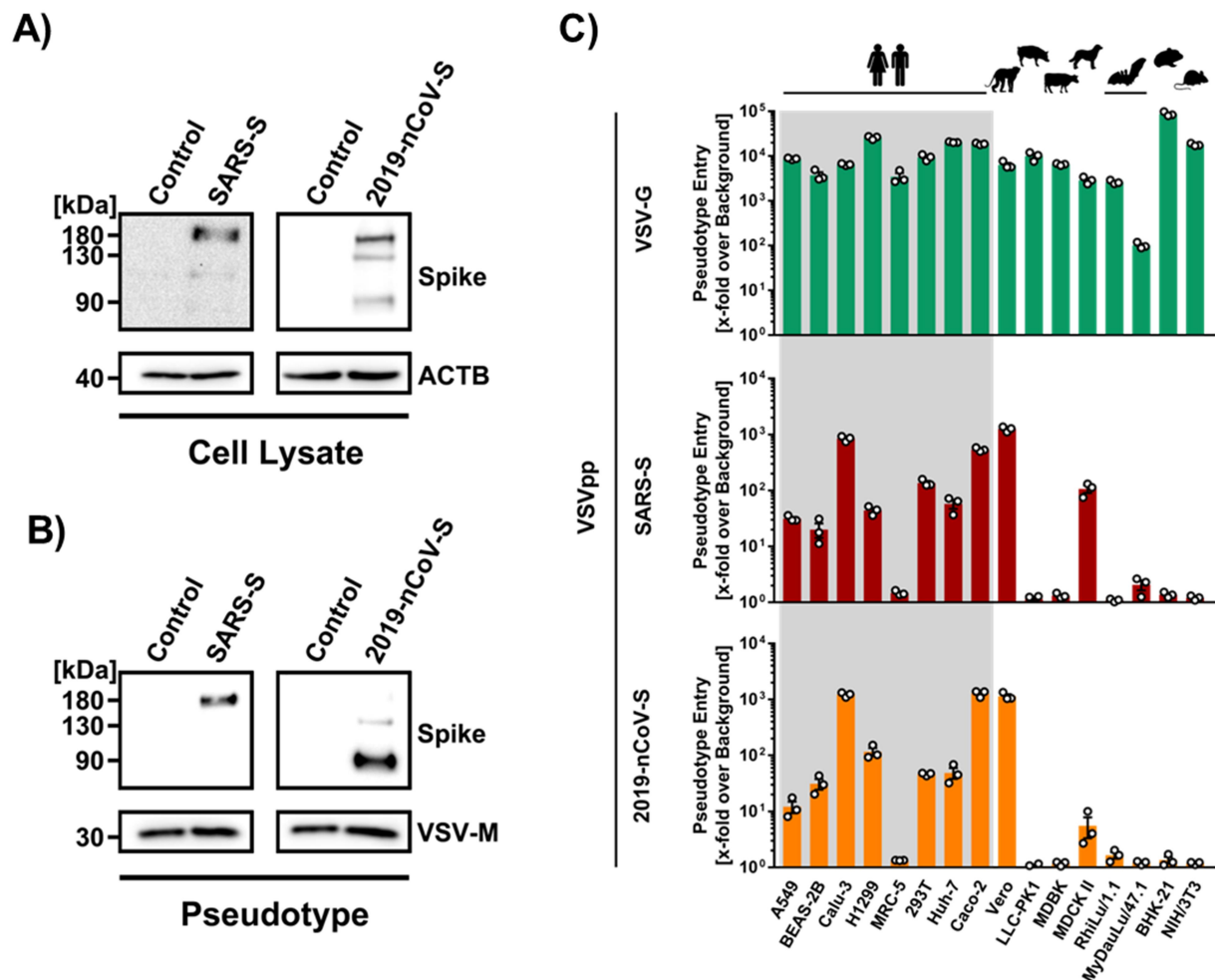
327

328

329

330

331

332

14

Fig. 1. 2019-nCoV-S and SARS-S facilitates entry into a similar panel of mammalian cell lines. Analysis of 2019-nCoV-S expression (**A**) and pseudotype incorporation (**B**) by Western blot. Representative blots from three experiments are shown. ß-Actin (cell lysates) and VSV-M (particles) served as loading controls. (C) Cell lines of human and animal origin were inoculated with pseudotyped VSV harboring VSV-G, SARS-S or 2019-nCoV-S. At 16 h postinoculation, pseudotype entry was analyzed. Shown are the combined data of three experiments. Error bars indicate SEM.

15
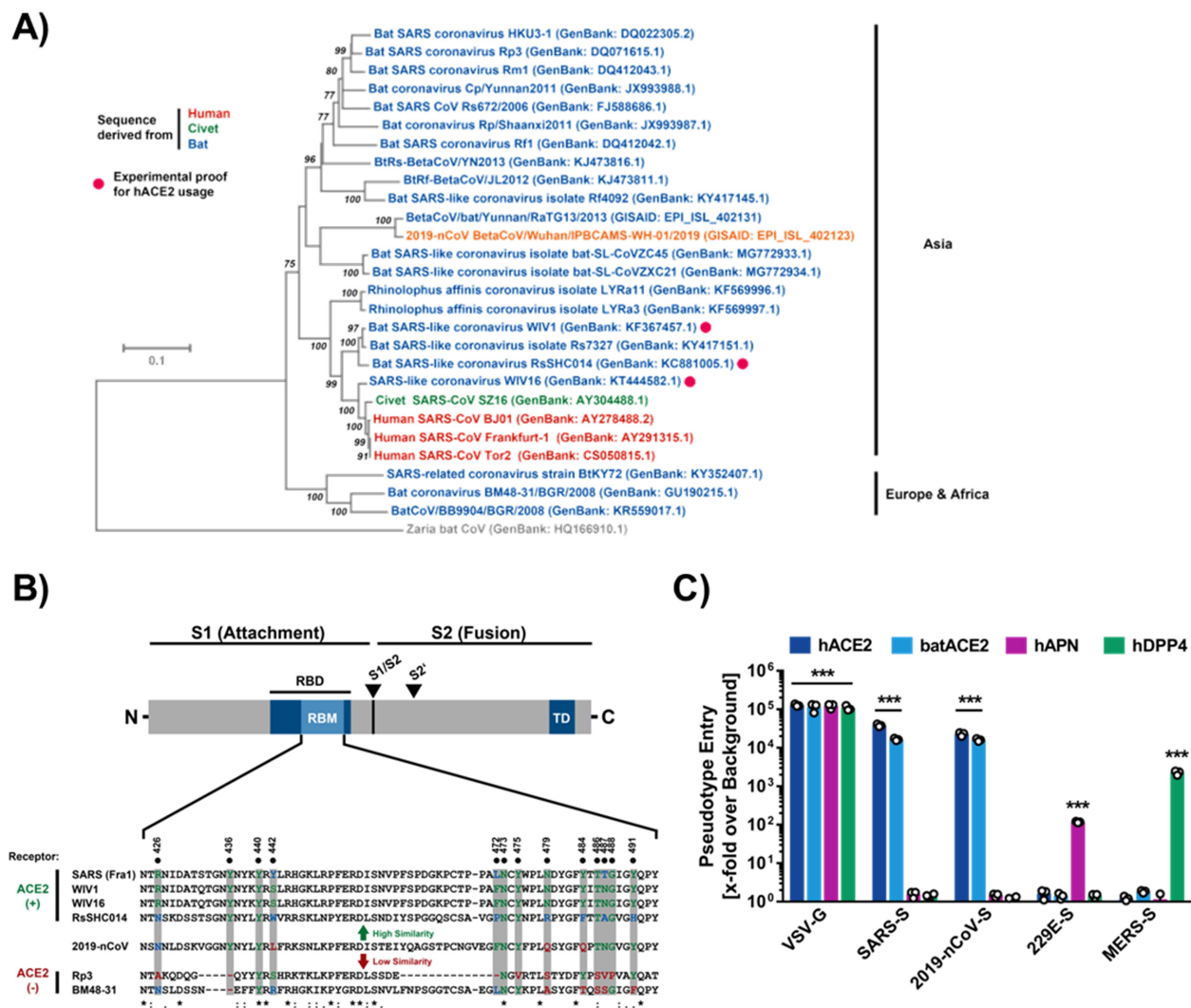
Fig. 2. 2019-nCoV-S utilizes ACE2 as cellular receptor. (**A**) The S protein of 2019-nCoV clusters phylogenetically with S proteins of known bat-associated betacoronaviruses (see also SI Figure 1 for more details). (**B**) Alignment of the receptor binding motif of SARS-S with corresponding sequences of bat-associated betacoronavirus S proteins that are able or unable to use ACE2 as cellular receptor reveals that 2019-nCoV possesses amino acid residues crucial for ACE2 binding. (**C**) 293T cells transiently expressing ACE2 of human (dark blue) or bat (light blue) origin, human APN (purple) or hDPP4 (green) were inoculated with pseudotyped VSV harboring VSV-G, SARS-S, 2019-nCoV-S, MERS-S or 229E-S. At 16 h postinoculation, pseudotype entry was analyzed. The average of three independent experiments is shown. Error bars indicate SEM.
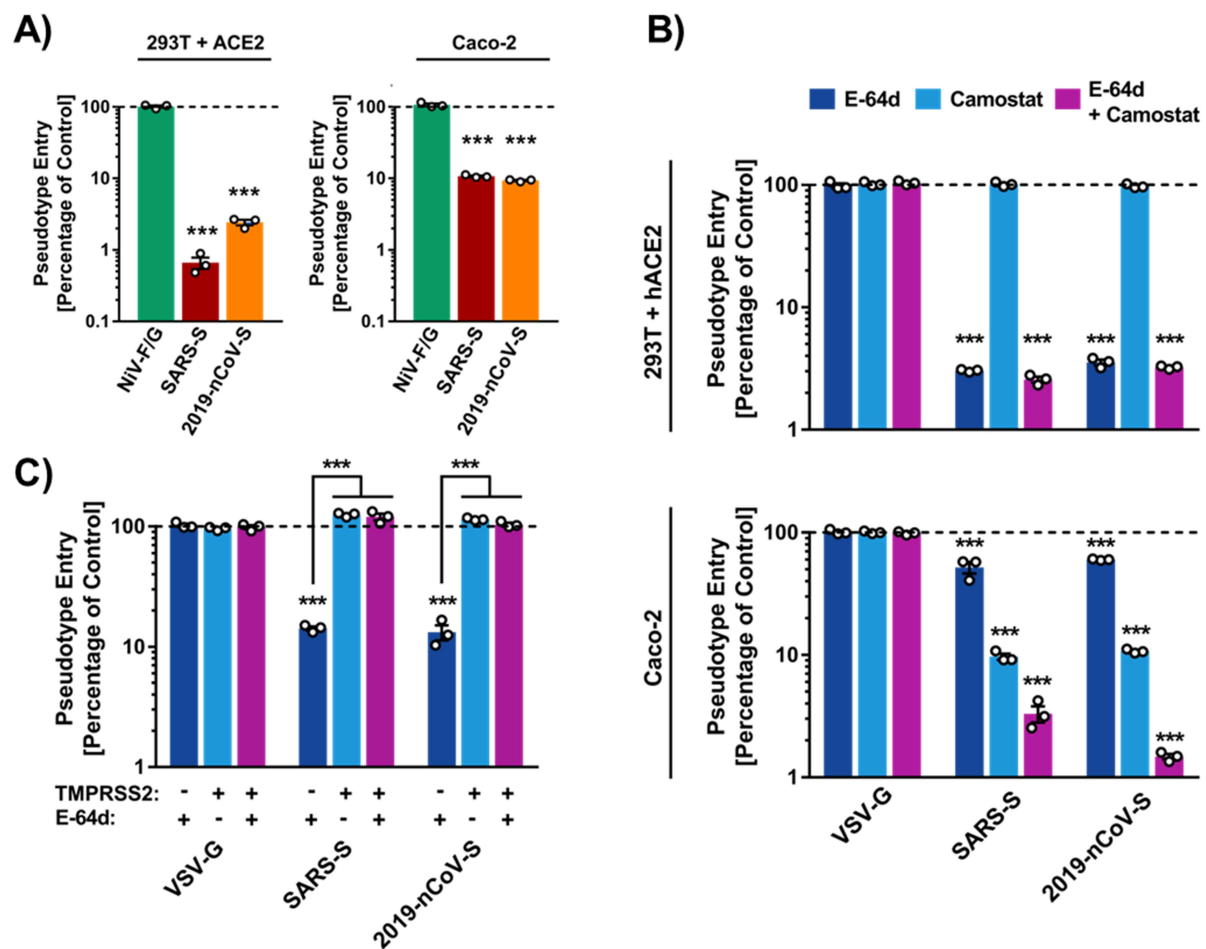
16

Fig. 3. 2019-nCoV-S employs TMPRSS2 for S protein priming. Ammonium chloride (**A**), E64d (CatB/L inhibitor) (**B**) and/or camostat (TMPRSS2 inhibitor) (**B**) were added to the indicated target cells before transduction with pseudotypes bearing the indicated glycoproteins. (**C**) 293T cells transiently expressing ACE2 alone or in combination with TMPRSS2 were incubated with CatB/L inhibitor E64d or PBS as control and inoculated with pseudotypes bearing the indicated viral surface proteins. The average of three independent experiments is shown in panels A-C. Error bars indicate SEM. Statistical significance was tested by two-way ANOVA with Dunnett posttest.
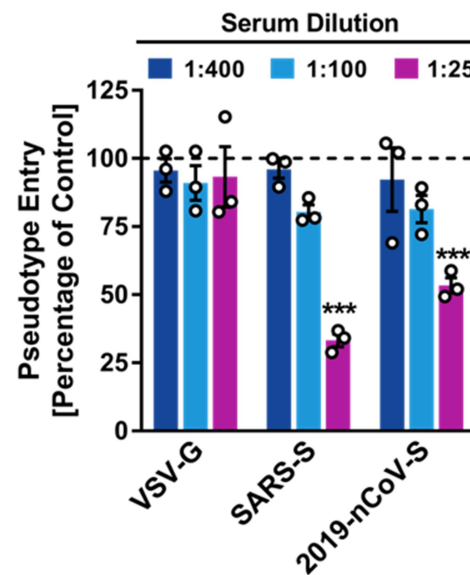
368

Fig. 4. Serum from a convalescent SARS patient cross-neutralizes 2019-nCoV-S-driven

entry. Pseudotypes harboring the indicated viral surface proteins were incubated with different

dilutions of serum from a convalescent SARS patient and subsequently inoculated onto 293T

cells that transiently express ACE2 in order to evaluate cross-neutralization. The results from a

representative experiment with triplicate samples are shown and were confirmed in a separate

experiment. Error bars indicate SD. Statistical significance was tested by two-way ANOVA with

Dunnett posttest.

376

1   **Supplementary Materials**

2

3   **Cell Culture**

4   All cell lines were incubated at 37 °C and 5 % CO_2 in a humidified atmosphere. 293T (human,
5   kidney), BHK-21 (Syrian hamster, kidney cells), Huh-7 (human, liver), LLC-PK1 (pig, kidney),
6   MRC-5 (human, lung), MyDauLu/47.1 (Daubenton's bat [*Myotis daubentonii*], lung), NIH/3T3
7   (Mouse, embryo), RhiLu/1.1 (Halcyon horseshoe bat [*Rhinolophus alcyone*], lung), Vero
8   (African green monkey, kidney) cells were incubated in Dulbecco's' modified Eagle medium
9   (PAN-Biotech). Calu-3 (human, lung), Caco-2 (human, colon), MDBK (cattle, kidney) and
10   MDCK II (Dog, kidney) cells were incubated in Minimum Essential Medium (ThermoFisher
11   Scientific). A549 (human, lung), BEAS-2B (human, bronchus) and NCI-H1299 (human, lung)
12   cells were incubated in DMEM/F-12 Medium with Nutrient Mix (ThermoFisher Scientific). All
13   media were supplemented with 10 % fetal bovine serum (Biochrom), 100 U/ml of penicillin and
14   0.1 mg/ml of streptomycin (PAN-Biotech), 1x non-essential amino acid solution (10x stock,
15   PAA) and 10 mM sodium pyruvate solution (ThermoFisher Scientific). For seeding and
16   subcultivation, cells were first washed with phosphate buffered saline (PBS) and then incubated
17   in the presence of trypsin/EDTA solution (PAN-Biotech) until cells detached. Transfection was
18   carried out by calcium-phosphate precipitation.

19

20   **Plasmids**

21   Expression plasmids for vesicular stomatitis virus (VSV, serotype Indiana) glycoprotein (VSV-
22   G), SARS-S (derived from the Frankfurt-1 isolate) with or without a C-terminal HA epitope tag,
23   HCoV-229E-S, MERS-S, human and bat angiotensin converting enzyme 2, human
24   aminopeptidase N, human dipeptidyl-peptidase 4 and human TMPRSS2 have been described
25   elsewhere (*1-6*). For generation of the expression plasmids for 2019-nCoV-S with or without a C-
26   terminal HA epitope tag we PCR-amplified the coding sequence of a synthetic, codon-optimized
27   (for human cells) 2019-nCoV-S DNA (GeneArt Gene Synthesis, ThermoFisher Scientific) based
28   on the publicly available protein sequence in the National Center for Biotechnology Information
29   database (NCBI Reference Sequence: YP_009724390.1) and cloned in into the pCG1 expression
30   vector via BamHI and XbaI restriction sites.

31

32   **Pseudotyping of VSV and transduction experiments**

33   *Pseudotyping*: VSV pseudotypes were generated according to a published protocol (*7*).In brief,
34   293T transfected to express the viral surface glycoprotein under study were inoculated with a
35   replication-deficient VSV vector that contains expression cassettes for eGFP (enhanced green

36 fluorescent protein) and firefly luciferase instead of VSV-G the open reading frame, VSV*ΔG-
37 fLuc (kindly provided by Gert Zimmer, Institute of Virology and Immunology,
38 Mittelhäusern/Switzerland). After an incubation period of 1 h at 37 °C, the inoculum was
39 removed and cells were washed with PBS before medium supplemented with anti-VSV-G
40 antibody (I1, mouse hybridoma supernatant from CRL-2700; ATCC) was added (no antibody
41 was added to cells expressing VSV-G). Pseudotype particles ware harvested 16 h postinoculation,
42 clarified from cellular debris by centrifugation and used for experimentations.

43 *Transduction of target cells*: Target cells were grown in 96-well plates until they reached 50-75
44 % confluency before they were inoculated with the respective pseudotype vectors. For
45 experiments addressing the search for the 2019-nCoV receptor cells were transfected with
46 expression plasmids 24 h in advance. For experiments involving ammonium chloride (final
47 concentration 50 mM) and protease inhibitors (E-64d, 25 µM; camostat mesylate, 100 µM),
48 target cells were treated with the respective chemical 2 h in advance. For neutralization
49 experiments, pseudotypes were pre-incubated for 30 min at 37 °C with different serum dilutions.
50 Transduction efficiency was quantified 16 h posttransduction by measuring the activity firefly
51 luciferase in cell lysates.

52

Analysis of 2019-nCoV-S expression and particle incorporation by SDS-PAGE and immunoblot

55 *Preparation of whole cell lysates*: 293T cells were transfected with expression vectors for HA-
56 tagged 2019-nCoV-S or SARS-S , or empty expression vector (negative control). The culture
57 medium was replaced at 16 h posttransfection and the cells were incubated for an additional 24 h.
58 Then, the culture medium was removed and cells were washed once with PBS before 2x SDS-
59 sample buffer (0.03 M Tris-HCl, 10% glycerol, 2% SDS, 0.2% bromophenol blue, 1 mM EDTA)
60 was added and cells were incubated for 10 min at room temperature. Next, the samples were
61 heated for 15 min at 96 °C and subjected to SDS-PAGE and immunoblotting. *Preparation of*
62 *pseudotype particle lysates*: 1 ml of the respective VSV pseudotype were loaded on a 20 % (w/v)
63 sucrose cushion (volume 40 µl) and subjected to high-speed centrifugation (25.000 g for 120 min
64 at 4 °C). Thereafter, 1 ml of supernatant was removed and the residual volume was mixed with
65 40 µl of 2x SDS-sample buffer, heated for 15 min at 96 °C and subjected to SDS-PAGE and
66 immunoblotting

67 After protein transfer, nitrocellulose membranes were blocked in 5 % skim milk (in PBS
68 containing 0.05 % Tween-20, PBS-T) for 1 h at room temperature and then incubated over night
69 at 4 °C with the primary antibody (diluted in PBS-T). Following three washing intervals of 10
70 min in PBS-T the membranes were incubated for 1 h at room temperature with the secondary
71 antibody (diluted in PBS-T), before the membranes were washed and imaged using an in in
72 house-prepared enhanced chemiluminescent solution (0.1 M Tris-HCl [pH 8.6], 250 µg/ml
73 luminol, 1 mg/ml para-hydroxycoumaric acid, 0.3 % H_2O_2) and the ChemoCam imaging system

2

74 along with the ChemoStar Professional software (Intas Science Imaging Instruments GmbH). The
75 following primary antibodies were used: Mouse anti-HA tag (Sigma-Aldrich, H3663, 1:2,500),
76 mouse anti-ß-actin (Sigma-Aldrich, A5441, 1:2,000), mouse anti-VSV matrix protein (Kerafast,
77 EB0011, 1:2,500). As secondary antibody we used a peroxidase-coupled goat anti-mouse
78 antibody (Dianova, 115-035-003, 1:10000).

79

Phylogenetic analysis

81 Phylogenetic analysis (neighbor-joining trees) was performed using the MEGA7.0.26 software.
82 Reference sequences were obtained from the National Center for Biotechnology Information and
83 GISAID (Global Initiative on Sharing All Influenza Data) databases. Reference numbers are
84 indicated in the figures.

85

Statistical analysis

87 One-way or two-way analysis of variance (ANOVA) with Dunnett's or Sidaks' posttest was used
88 to test for statistical significance. Only p values of 0.05 or lower were considered statistically
89 significant ($p > 0.05$ [ns, not significant], $p \leq 0.05$ [*], $p \leq 0.01$ [**], $p \leq 0.001$ [***]). For all
90 statistical analyses, the GraphPad Prism 7 software package was used (GraphPad Software).

91

Supplementary references

93

94 1. C. Brinkmann *et al.*, The glycoprotein of vesicular stomatitis virus promotes release of
95 virus-like particles from tetherin-positive cells. *PLoS One* **12**, e0189073 (2017).
96 2. M. Hoffmann *et al.*, Differential sensitivity of bat cells to infection by enveloped RNA
97 viruses: coronaviruses, paramyxoviruses, filoviruses, and influenza viruses. *PLoS One* **8**,
98 e72942 (2013).
99 3. H. Hofmann *et al.*, Human coronavirus NL63 employs the severe acute respiratory
100 syndrome coronavirus receptor for cellular entry. *Proc Natl Acad Sci U S A* **102**, 7988-
101 7993 (2005).
102 4. S. Bertram *et al.*, TMPRSS2 and TMPRSS4 facilitate trypsin-independent spread of
103 influenza virus in Caco-2 cells. *J Virol* **84**, 10016-10025 (2010).
104 5. S. Gierer *et al.*, The spike protein of the emerging betacoronavirus EMC uses a novel
105 coronavirus receptor for entry, can be activated by TMPRSS2, and is targeted by
106 neutralizing antibodies. *J Virol* **87**, 5502-5511 (2013).
107 6. H. Kleine-Weber *et al.*, Mutations in the Spike Protein of Middle East Respiratory
108 Syndrome Coronavirus Transmitted in Korea Increase Resistance to Antibody-Mediated
109 Neutralization. *J Virol* **93**, (2019).

110   7.   M. Berger Rentsch, G. Zimmer, A vesicular stomatitis virus replicon-based bioassay for
111   the rapid and sensitive determination of multi-species type I interferon. *PLoS One* **6**,
112   e25858 (2011).

113

114   **Supplementary figure S1**

115
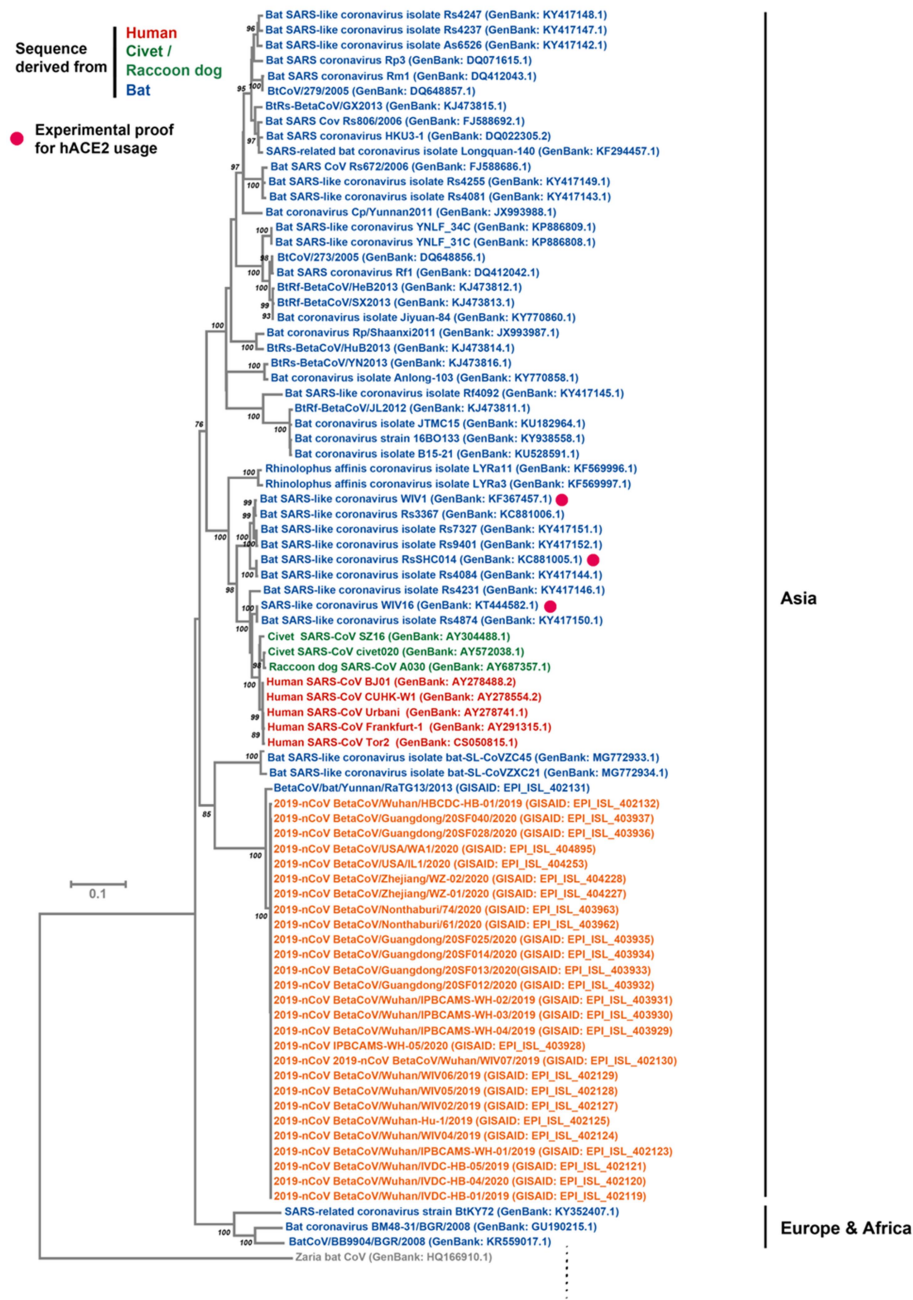
116   **Legend to supplementary figure S1.** Phylogenetic analysis (neighbor-joining tree) of spike

117   protein sequences. Small numbers indicate bottstrap values (only values higher that 75 are

118   shown).

119

120

121

122

123

124